Prog. Oceanog. Vol. 14, pp. 103-127, 1985.
Printed in Great Britain.

0079-6611/85 $0.00 + .50
Pergamon Press Ltd.

Estimates of the Mean Circulation in the Deep (>2,000m) Layer of the Eastern North Atlantic

R. R. DICKSON,* W. J. GOULD,† T. J. MÜLLER‡ and C. MAILLARD§

**Ministry of Agriculture, Fisheries and Food, Directorate of Fisheries Research, Fisheries Laboratory, Lowestoft, Suffolk NR33 0HT, U.K.*

†Institute of Oceanographic Sciences, Wormley, Godalming, Surrey GU8 5UB, U.K.

‡Institute für Meereskunde, Universität Kiel, D-2300 Kiel 1, F.R.G.

§CNEXO, Centre Oceanologique de Bretagne, 29 N Plouzane, 29273 Brest Cedex, France

Abstract–A total of 131 current meter records of between 6 and 24 month duration are analysed to describe the deep flow field of the eastern North Atlantic from 19° to 54°N and from the Continental Slope to the Mid Atlantic Ridge. Mean flows are weak and may be statistically indeterminate in some records and locations, but appear to indicate cyclonic circulations around the Iberia and Porcupine abyssal plains with a generally southward flow along the Mid Atlantic ridge and a deep northward slope current (where measurements exist) along the eastern boundary. The deepest inflow to the north-eastern basin that has been identified to date takes place through the Discovery Gap of > 4,700 m sill-depth at 37°25'N 15°45'W in the Azores–Portugal ridge. South of that ridge, observations are sparse and no systematic circulation is yet evident. These observations are discussed in relation to recent geostrophic estimates of the deep circulation.

1. INTRODUCTION

PRIOR to 1976 the deep flow field of the eastern North Atlantic was virtually undescribed, and the very few direct current measurements available were severely restricted both in distribution and duration. Since then, new initiatives in support of a wide range of scientific interests have contributed a total data-set of some 200 meter-years of Eulerian current meter records (all depths). Many of the records are of recent origin and have yet to be fully analysed.

The key initiative was that of the North East Atlantic Dynamics Study (NEADS) subgroup of SCOR Working Group 34 which, from November 1976, maintained a large-scale incoherent array of full-depth moorings in the eastern basin. These were specifically designed to provide records of 2 yr duration from widely-spaced sites remote from the influence of major topographic features (e.g. islands, continental slopes). The NEADS plan and participants are described in ANON, 1976. Though the geographic spread of measurements has extended to most areas of the basin since the main period of the NEADS programme, the NEADS records still stand out by virtue of their unusually long duration and full-depth coverage.

The longest records are of particular importance to the present paper. The vast majority of eastern basin measurements, including those of the NEADS programme, were designed primarily to provide information on the eddy field, (particularly the large-scale spatial variability of eddy kinetic energy, the dominant time-scales of eddy motions and their vertical structure), and the kinematics and statistics of the eddy field have already been partly described (DICKSON, 1983; GOULD, 1983; DICKSON, GOULD, GURBUTT and KILLWORTH,

TABLE 1. FLOW STATISTICS FOR 131 DEEP CURRENT METER RECORDS FROM THE EASTERN NORTH ATLANTIC. u AND v DENOTE EASTWARD AND NORTHWARD RESPECTIVELY, DATA ARE LOW PASS FILTERED TO REMOVE PERIODS LOWER THAN 2 DAY (NOMINAL), TIME AVERAGES DENOTED BY OVERBAR, DEVIATIONS FROM THESE AVERAGES BY A PRIME; $\overline{u'^2}$ AND $\overline{v'^2}$ ARE THE VARIANCES IN u AND v, K_E IS THE EDDY KINETIC ENERGY PER UNIT MASS $[\frac{1}{2}(\overline{u'^2}+\overline{v'^2})]$, K_M IS THE KINETIC ENERGY PER UNIT MASS OF THE MEAN FLOW $[\frac{1}{2}(\bar{u}^2+\bar{v}^2)]$, $\overline{u'v'}$ IS THE EDDY MOMENTUM FLUX, AND THE 'STABILITY FACTOR' IS THE RATIO OF MEAN VECTOR TO MEAN SCALAR SPEEDS EXPRESSED AS A PERCENTAGE. THE STANDARD ERROR CALCULATION IS DESCRIBED IN THE TEXT

Identifier	Latitude N (° ′)	Longitude W (° ′)	Water depth (m)	Sampling depth (m)	Duration (days)	$\bar{u}$ (cm s⁻¹)	$\bar{v}$ (cm s⁻¹)	$\overline{u'v'}$ (cm² s⁻²)	Stability factor (%)	$\overline{u'^2}$ (cm² s⁻²)	$\overline{v'^2}$ (cm² s⁻²)	K_E (cm² s⁻²)	K_M (cm² s⁻²)	Std. err. u (cm s⁻¹)	Std. err. v (cm s⁻¹)	Source
NEADS network																
NEADS 1	33 06	21 50	5270	3050	721	−0.4	−0.52	−1.1	29	2.5	3.9	3.2	0.21	0.51	0.62	IFMK (Muller)
				4780	345	0.3	−1.1	−1.2	45	2.6	4.8	3.7	0.65	0.42	0.76	
~ NEADS 1	33 07	20 03		4638	225	−0.29	0.20			2.41	2.21	2.31	0.09			IOS (Saunders)
				5284	225	−0.11	0.06			3.14	2.79	2.96	0.06			
NEADS 2	37 59	16 54	5550	3168	689	0.4	0.1	0.3	41	0.9	0.6	0.8	0.09	0.35	0.22	IFMK (Muller)
				4181	465	1.1	0.3	0.2	77	1.0	0.9	0.9	0.65	0.37	0.33	
				5079	146	0.7	1.1	0.1	88	0.4	0.5	0.4	0.85	0.13	0.15	
NEADS 2½	40 31	17 19	5310	2945	202	−0.7	−0.0	−0.1	50	0.9	0.8	0.8	0.25	0.50	0.30	IFMK (Muller)
				4050	242	−0.5	0.1	−0.1	71	0.1	0.3	0.2	0.13	0.08	0.12	
NEADS 3	42 00	14 00	5330	3000	470	−0.15	0.30	0.60		6.27	5.12	5.70	0.06			IOS (Gould)
				4000	700	−0.94	0.19	0.23		6.11	4.62	5.37	0.46			
NEADS 3½	41 30	20 00	3700	3100	150	−0.26	0.04	0.90		1.04	1.43	1.24	0.03			IOS (Gould)
NEADS 4	41 00	25 00	3634	3000	466	−0.79	−0.92	0.94		3.07	4.14	3.61	0.74			IOS (Gould)
				3500	688	−0.90	−0.54	−1.24		4.26	4.36	4.31	0.55			
NEADS 5	46 00	17 00	4756	3000	485	−0.23	0.67	0.24		3.04	2.03	2.53	0.25			IOS (Gould)
NEADS 5	46 06	17 09	4760	4050	362	−0.65	0.77	0.39	63	0.98	1.05	1.02	0.50	0.26	0.21	MAFF (Dickson)
				4200	362	−0.52	0.62	0.28	65	0.56	0.71	0.63	0.33	0.18	0.16	
				4710	307	−0.64	0.82	0.52	62	1.57	0.87	1.22	0.55	0.33	0.26	
NEADS 6(1)	52 28.7	17 43.9	4100	3050	239	0.61	−0.10	0.33	16	9.78	8.27	9.03	0.19	0.60	0.43	MAFF (Dickson)
				4050	239	−1.30	−0.25	1.26	26	14.75	14.07	14.41	0.88	0.63	0.56	
NEADS 6(2)	52 27.8	17 42.0	4121	3071	343	0.09	0.11	−1.09	4	11.90	7.54	9.72	0.01	0.47	0.33	MAFF (Dickson)
NEADS 6(3)	52 27.8	17 42.6	4124	3047	248	−0.94	0.83	−4.65	24	19.15	16.52	17.84	0.79	0.95	0.54	MAFF (Dickson)
				4074	363	−2.32	1.10	−3.27	37	25.87	31.10	28.48	3.30	0.70	0.62	
NEADS 6(4)	52 25.1	17 44.8	4187	3137	365	0.24	−0.11	−8.32	5	24.49	17.62	21.05	0.03	0.74	0.60	MAFF (Dickson)
				4137	365	−1.09	−0.03	−9.32	14	46.24	39.05	42.65	0.58	0.98	0.83	
NEADS 6(5)	52 27.7	17 43.8	4107	3057	342	−0.68	−0.61	−0.13	29	7.92	6.81	7.36	0.42	0.45	0.31	MAFF (Dickson)
NEADS 6(6) ≡ mooring 82-09 (see below)																
NEADS 7	47 00	10 00	4995	3000	260	−0.17	0.02					1.2	0.01			COB (Colin de Verdiere)
				4000	732	0.37	−0.33	−0.60		2.33	1.91	2.1	0.12			
NEADS 11	34 50	23 00	5155	3030	592	0.50	0.47	0.4	56	0.97	0.65	0.81	0.23	0.22	0.17	IFMK (Muller)
				4720	214	2.28	2.20	3.0	92	4.5	4.3	4.4	5.02	0.71	0.65	
NEADS 12	30 56	20 23	4850	2970	213	0.14	−0.11	−0.3	12	1.2	1.4	1.3	0.01	0.42	0.40	IFMK (Muller)
				4690	213	0.31	−0.30	−0.3	25	1.6	1.8	1.7	0.09	0.46	0.42	

Porcupine Bank Slope																
81-07	52 30.2	15 25.9	2555	2505	210	−0.17	3.37	−2.23	93	1.85	4.87	3.36	5.69	0.22	0.34	MAFF (Dickson)
Celtic Sea Slope																
R	48 59.2	12 52.6	2099	2049	354	−0.30	2.21	−3.02	64	2.08	9.87	5.98	2.49	0.27	0.62	MAFF (Dickson)
80-02	47 15.5	09 58.2	4395	2995	344	0.41	0.44	0.15	46	1.05	0.70	0.88	0.18	0.22	0.15	MAFF (Dickson)
				3995	347	−0.31	0.41	0.16	30	1.47	1.98	1.73	0.13	0.21	0.26	
Meriadzek Terr.	47 35.0	08 25.0	2150	1995	170	−1.76	0.15						1.56			IOS (Gould)
Porcupine Abyssal Plain																
N	50 42.7	17 00.8	4754	3984	330	−0.86	1.64	3.61	41	9.17	15.27	12.22	1.71	0.72	0.85	MAFF (Dickson)
				4704	363	−1.27	2.20	2.53	53	8.67	13.82	11.24	3.21	0.67	0.77	
O	49 10.4	15 44.6	4820	3990	333	−0.42	2.25	−0.16	61	6.93	4.31	5.62	2.61	0.65	0.45	MAFF (Dickson)
				4770	298	−0.89	2.01	0.78	59	6.78	4.48	5.63	2.41	0.73	0.45	
P	47 59.5	14 06.4	4250	3750	357	0.51	−0.51	0.49	49	1.19	1.25	1.22	0.26	0.19	0.32	MAFF (Dickson)
				4200	357	0.92	−0.51	−1.04	59	1.83	2.17	2.00	0.55	0.22	0.28	
Q	47 13.6	12 12.8	4751	4701	349	−0.31	0.40	0.44	19	5.69	3.61	4.65	0.13	0.44	0.41	MAFF (Dickson)
Biogas 81-82	47 35.3	09 39.6	4310	4300	324	−0.48	1.35		69				1.03			COB (Vangriesheim)
Tourbillon 79-80																
1	46 59.7	14 49.6	4785	3030	237	0.22	0.97	−1.05		2.12	2.06	2.09	0.49			COB (Colin de Verdiere)
				4040	237	0.76	1.02	−1.17		3.13	2.45	2.79	0.81			(Ahrens)
2	46 59.6	14 35.9	4795	4040	237	0.80	0.31	−1.14		3.43	2.62	3.02	0.37			COB (Colin de Verdiere) (Ahrens)
3	47 11.5	14 50.9	4785	3000	237	−0.36	0.86	0.20		2.78	5.15	3.96	0.43			COB (Colin de Verdiere)
				4040	237	−0.36	0.91	0.68		2.88	4.43	3.66	0.48			(Ahrens)
4	47 00.6	15 04.3	4745	3040	237	−0.06	1.14	−1.66		1.91	3.95	2.93	0.65			COB (Colin de Verdiere)
				4070	237	1.00	0.95	−1.05		1.61	7.63	4.62	0.95			(Ahrens)
5	46 50.8	14 48.6	4785	3000	237	−1.06	0.65	−1.72		3.37	1.31	2.34	0.77			COB (Colin de Verdiere)
				4040	237	−0.40	0.05	−1.24		4.34	1.39	2.86	0.08			(Ahrens)
6	47 22.7	14 13.5	4807	2970	237	1.34	−0.68	−0.26		0.92	3.86	2.39	1.13			COB (Colin de Verdiere)
				4000	237	1.21	−0.35	−1.03		1.95	3.86	2.91	0.79			(Ahrens)
7	47 26.1	15 19.7	4795	3030	237	−0.79	0.38	2.74		6.28	4.42	5.35	0.38			COB (Colin de Verdiere)
				4070	237	−0.50	0.08	2.44		5.10	4.57	4.84	0.13			(Ahrens)
8	46 37.3	15 24.4	4690	3000	268	0.26	1.31	0.05	76	1.22	0.30	0.76	0.90	0.60	0.16	MAFF (Ramster)
				4000	268	1.69	2.06	0.90	92	2.34	0.78	1.56	3.55	0.71	0.31	
9	46 35.2	14 14.5	4780	3000	199	−0.94	1.35	0.22	83	0.86	0.83	0.85	1.36	0.26	0.27	MAFF (Ramster)
10	46 58.6	14 14.9	4775	4285	224	0.66	0.42						0.31			COB (Vangriesheim)
Edyloc 81/82	47 25.1	14 25.0	4785	2000	321	−2.01	−1.31			14.18	23.36	18.77	2.88			COB (Vangriesheim)
				4000	321	−1.98	−0.07			9.49	10.52	10.01	1.96			(Maillard)
				4775	321	−2.27	0.21			14.09	17.01	15.55	2.60			

Identifier	Latitude N (° ′)	Longitude W (° ′)	Water depth (m)	Sampling depth (m)	Duration (days)	$\bar{u}$ (cm s⁻¹)	$\bar{v}$ (cm s⁻¹)	$\overline{u'v'}$ (cm² s⁻²)	Stability factor (%)	$\overline{u'^2}$ (cm² s⁻²)	$\overline{v'^2}$ (cm² s⁻²)	K_E (cm² s⁻²)	K_M (cm² s⁻²)	Std. err. u (cm s⁻¹)	Std. err. v (cm s⁻¹)	Source
Topographic Array																
80-10	45 54.8	16 31.4	4025	3975	185	−0.99	−5.59	−2.11	95	3.50	7.49	5.50	16.11	0.45	0.74	MAFF (Gurbutt)
80-11	45 50.1	16 35.8	4349	3299	185	2.88	1.31	0.84	96	2.31	0.89	1.60	5.01	0.67	0.34	MAFF (Gurbutt)
				4299	185	1.02	2.01	1.24	73	1.61	4.57	3.09	2.53	0.41	0.53	
80-12	45 54.4	16 37.2	4280	2730	257	2.08	2.23	0.38	92	1.76	1.73	1.75	4.66	0.40	0.37	MAFF (Gurbutt)
				3480	135	0.86	2.58	−0.04	95	0.52	1.12	0.82	3.69	0.21	0.40	
				4230	257	0.36	3.09	0.59	93	0.96	3.68	2.32	4.83	0.22	0.47	
Charlie Gibbs F.Z.																
North 570	52 42.7	33 59.2	4311	4227	269	−4.1	−0.6			40.5	2.2	21.4	8.6			WHOI (Schmitz, Hogg)
571	52 53.7	35 31.0	2895	2835	270	−0.4	0.7			4.4	5.8	5.1	0.3			WHOI (Schmitz, Hogg)
572	52 46.1	35 30.0	3398	2528	270	−4.4	−1.6			34.2	9.0	21.6	11.0			WHOI (Schmitz, Hogg)
				3060	270	−3.8	−1.0			42.3	6.1	24.2	7.7			
				3360	270	−3.2	−2.1			34.4	11.1	22.8	7.3			
South A	52 11.8	30 58.2	3050	2500	247	0.34	0.46	0.60	15	20.80	0.66	10.73	0.16	0.92	0.13	MAFF (Dickson)
				3000	247	−0.77	0.29	0.11	73	0.62	0.27	0.44	0.34	0.13	0.06	
B	52 09.3	31 00.2	4027	2977	250	1.66	−0.10	8.88	24	60.08	7.22	33.65	1.38	2.17	0.48	MAFF (Dickson)
				3977	250	−3.31	−0.43	2.46	72	15.55	3.72	9.64	5.58	0.57	0.37	
C	52 05.6	30 57.5	3577	3527	247	2.66	−0.54	−0.47	91	3.84	0.52	2.18	3.69	0.31	0.12	MAFF (Dickson)
East Flanks MAR																
265	48 33	26 05	3717	2520	665	−1.1	0.6	−1.7	43	4.7	5.5	5.1	0.79	0.57	0.49	IFMK (Meinke)
266	44 26.4	26 05	3167	2479	390	−0.69	0.42	−2.16	29	5.54	3.88	4.71	0.32	0.66	0.52	IFMK (Meinke)
81-03/12	46 48.8	23 46.2	3992	2873	113	0.47	−0.67	−1.06	43	1.99	1.95	1.97	0.33	0.69	0.74	MAFF (Dickson)
				3945	373	−1.97	0.85	−1.03	82	3.24	1.54	2.39	2.30	0.47	0.23	
81-04/11	47 07.3	21 42.9	4532	3374	372	−1.92	−1.11	−1.38	75	2.57	2.86	2.71	2.47	0.54	0.42	MAFF (Dickson)
				4485	372	−2.54	−0.83	−1.00	80	4.17	3.20	3.68	3.58	0.44	0.34	
81-05/10	47 26.9	20 11.2	4540	3556	371	−3.23	−0.57	0.57	86	6.72	1.95	4.33	5.37	0.58	0.34	MAFF (Dickson)
				4493	371	−4.27	−0.17	1.20	82	15.09	3.49	9.29	9.13	0.89	0.32	
81-06/09	47 55.3	18 32.9	4527	3591	371	0.28	−1.71	0.41	81	1.69	1.60	1.65	1.51	0.33	0.29	MAFF (Dickson)
				4480	371	−0.87	−2.83	1.32	87	2.58	4.20	3.39	4.39	0.38	0.44	
Rockall Array																
82-07/16	53 25.4	19 01.8	2498	2453	368	3.57	1.03	−2.81	48	33.98	33.47	33.72	6.91	1.01	0.93	MAFF (Dickson)
82-08/15	52 58.9	18 23.6	3162	3117	367	−3.92	−4.39	35.95	68	32.55	49.26	40.91	17.32	0.81	1.01	MAFF (Dickson)
82-09	52 27.3	17 42.9	4135	2346	366	0.05	−0.15	−2.11	3	16.79	13.51	15.15	0.01	0.95	0.61	MAFF (Dickson)
				3109	366	−0.51	0.47	−1.32	12	22.11	21.96	22.00	0.24	0.67	0.55	
				3910	366	−1.21	1.55	−2.24	26	37.83	37.69	37.76	1.93	0.84	0.69	
82-10/18	51 54.2	17 38.7	4470	3556	368	−1.59	0.36	−6.20	29	27.02	18.06	22.54	1.33	0.98	0.63	MAFF (Dickson)
				4425	368	−4.19	1.31	−7.21	55	45.10	24.73	34.91	9.65	2.45	0.71	
MAR–Rockall Gap																
82-11	50 49.7	20 31.4	4314	4085	241	−0.14	3.69	−0.03	93	1.04	7.11	4.07	6.83	0.13	0.80	MAFF (Dickson)
				4269	368	−0.32	4.93	−0.08	88	2.47	16.06	9.26	12.22	0.26	0.85	

Kings Trough																
80-14	42 25.5	20 35.1	4108	3058	370	−0.36	−0.51	0.91	36	2.29	1.12	1.71	0.20	0.44	0.32	MAFF (Gurbutt)
				4058	370	−0.55	−0.68	1.90	29	6.54	3.52	5.03	0.38	0.54	0.44	
80-15	41 44.9	21 57.0	3840	3000	369	−0.39	−1.79	0.43	64	3.51	3.12	3.32	1.68	0.39	0.37	MAFF (Gurbutt)
				3790	369	−0.64	−2.45	0.55	78	2.35	3.98	3.16	3.20	0.16	0.43	
80-16	41 38.6	21 08.7	3568	3518	367	2.57	0.05	−0.90	79	5.87	1.56	3.71	3.31	1.06	0.46	MAFF (Gurbutt)
NE of Azores																
G	41 01.1	26 26.4	2637	2587	342.	Modal direction only				–	–	–	–	–	–	MAFF (Dickson)
H	40 59.6	25 47.0	3364	2314	317	Modal direction only				–	–	–	–	–	–	MAFF (Dickson)
				3314	229	Modal direction only				–	–	–	–	–	–	
J	41 00.3	24 27.1	3753	2703	174	−0.20	0.63	−0.04	70	0.39	0.25	0.32	0.22	0.27	0.16	MAFF (Dickson)
K	41 01.5	24 04.5	3395	2345	257	0.16	0.31	0.01	55	0.25	0.12	0.18	0.06	0.17	0.06	MAFF (Dickson)
				3345	339	−0.62	0.30	−0.09	65	0.50	0.47	0.48	0.24	0.10	0.08	
L	41 00.4	23 17.8	4096	4046	340	0.29	−0.64	0.51	40	1.39	2.18	1.79	0.25	0.20	0.23	MAFF (Dickson)
Azores–Portugal ridge																
310	37 21.2	15 45.7	5046	5027	340	3.20	2.0						7.12			IOS (Gould/Saunders)
Madeira AP																
81-14	29 59.4	27 21.3	4912	3935	181	0.30	−0.74	−0.21	53	1.82	1.43	1.63	0.32	0.43	0.39	MAFF (Gurbutt/Dickson)
				4862	256	1.26	−0.82	−1.18	59	3.11	2.55	2.83	1.12	0.55	0.54	
81-15	30 00.5	25 21.5	5419	4366	257	−0.38	−0.41	0.72	33	2.55	0.57	1.56	0.16	0.67	0.26	MAFF (Gurbutt/Dickson)
81-16	30 19.5	23 22.0	5296	3195	252	0.32	0.72	0.11	57	1.23	0.59	0.91	0.31	0.33	0.21	MAFF (Gurbutt/Dickson)
				4246	252	0.81	1.58	−0.20	73	2.89	1.03	1.96	1.57	0.53	0.26	
				5246	252	0.85	1.68	0.11	75	2.98	1.12	2.05	1.78	0.52	0.25	
81-17	31 00.5	21 50.4	5027	3996	252	−0.11	0.03	0.15	7	1.44	1.84	1.64	0.01	0.30	0.48	MAFF (Gurbutt/Dickson)
				4977	252	−0.10	0.27	0.27	14	2.18	2.57	2.38	0.04	0.38	0.48	
81-18	32 00.1	20 00.2	4511	3480	252	−0.11	0.66	−1.12	28	0.82	6.52	3.67	0.23	0.27	0.89	MAFF (Gurbutt/Dickson)
				4461	252	−0.40	0.78	−3.86	21	7.66	14.39	11.03	0.38	0.76	1.03	
POLYMODE III B																
623	27 24.8	41 07.7	4251	3927	345	0.05	0.36			1.13	1.28	1.21	0.07			MIT (Wunsch)
624	27 17.5	40 45.5	4372	4028	173	0.41	−0.07			0.65	0.46	0.60	0.09			MIT (Wunsch)
625	27 14.5	40 21.1	4723	3990	343	0.55	0.50			0.47	0.40	0.40	0.30			MIT (Wunsch)
626	26 52.7	41 12.8	4315	4014	342	1.00	−0.57			2.45	0.78	1.62	0.66			MIT (Wunsch)
649	27 25	41 09	4268	4018	486	0.1	0.8						0.33			MIT (Wunsch)
Canary AP																
CV1	24 49.6	25 02.9	5200	5190	178	−0.15	0.95			0.91	2.61	1.76	0.46			COB (Vangriesheim)
CV2	19 14.0	29 47.7	4885	4785	185	−1.12	−0.66			0.61	1.38	0.99	0.84			COB (Vangriesheim)
				4875	185	−1.38	−0.58			0.81	1.54	1.17	1.12			

1982). The provision of reliable estimates of the mean circulation was of secondary importance in the planning of these moorings and arrays. As will be shown below, though the typical record lengths of 9 months to 1 yr are mostly adequate to describe the variances of the flow field, they provide a less reliable estimate of the means.

This paper will discuss estimates of the mean circulation for the 131 records from the deep layer (> 2,000 m) of the eastern Atlantic, and will attempt to assess their statistical reliability. The paper's main aim is not to identify the cause or causes of the abyssal circulation in the eastern basin, but is to evaluate whether, and where, a reliable mean circulation can be said to exist.

The full data set, its sources and the derived statistics referred to in the text are listed in Table 1. All data are from moorings with subsurface buoyancy; thus records are not contaminated by wave action and data are comparable regardless of current meter type (SWALLOW, 1975).

2. STANDARD ERROR ESTIMATES

The two statistics commonly computed from low-passed current meter records are (a) the mean values of east (u) and north (v) components and (b) the kinetic energy per unit mass of the fluctuating component $[K_E = \frac{1}{2}(\text{var.}\, u + \text{var.}\, v)]$.

Errors in our estimates of both means and variances are a function of record length and of the dominant periodicity of the record. For a simple sinusoid for example it can be shown that the errors in variance estimates decay partly as $1/T$, and partly as $1/T^2$, where T is the record length. They thus converge much more rapidly than the error in the mean, which decays like $1/T$ and has the same periodicity (τ) as the original signal. This general characteristic is compounded in the north-east Atlantic by the shortness of available records (9 months to 1 yr on average) and the smallness of the means compared with the fluctuating component. (DICKSON, 1983 e.g. his Fig. 3n). Figure 1 indicates that 67–69% of mean u and v components in the available records and 45% of their resultant vectors are less than 1 cm s^{-1}. In this section, these means are compared with their corresponding standard error estimates for 85 of the deep eastern basin records.

The standard error in a mean is a function of the variance divided by the number of independent time periods in the record. In a data series of n terms, sampling interval Δt and dominant periodicity τ, DAVIS (1976) shows that the number of degrees of freedom $\alpha \neq n\Delta t/\tau$, but $\alpha = n\Delta t/\tau_i$, where τ_i is defined as an *integral time scale.* LUYTEN (1982) follows the argument of FLIERL and MCWILLIAMS (1977) to derive his equation for an integral time scale:

$$\tau_i = \sum_{i=0}^{N} C(i\Delta t)\, \Delta t,$$

where $N\Delta t$ is the lag for which the autocorrelation $C(i\Delta t)$ is at its first zero crossing. The standard error in the mean ($\sqrt{\epsilon}$) is then calculated from the expression

$$\epsilon = \frac{2\,\tau_i \sigma^2}{n\Delta t}, \text{ where } \sigma^2 \text{ is the variance.}$$

In the present paper, Luyten's method is accepted as valid, though it remains far from clear whether this method yet represents the optimal approach. Summation of the autocorrelation function to first zero crossing poses problems for records with very long time-scales where the autocorrelation function may not become negative within the available number of lags. On

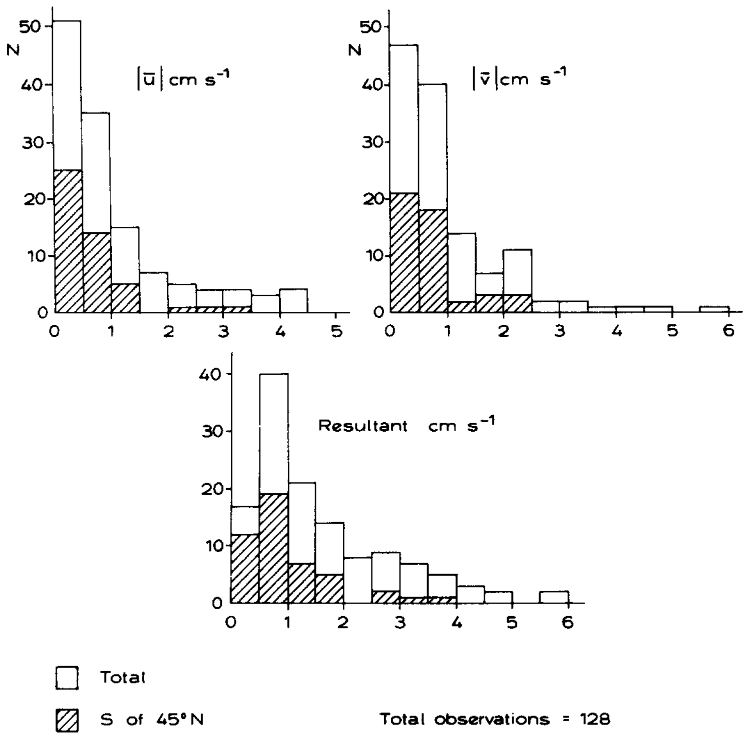

FIG. 1. Numbers of observations of $|\bar{u}|$, $|\bar{v}|$ and their resultant in each 0.5 cm s^{-1} band of mean speed.

the other hand, a full summation to include all lags of the autocorrelation function may be equally problematic in the case of records with a well defined periodicity, since in these cases, the estimates of integral time scale τ_i will be dependent on the number of lags. A compromise solution might involve the summation of all terms of the autocorrelation function but applying a linear taper, thus making use of the full record while reducing the influence of terms at large lags. (See HENDRY, 1982.)

In fact the method of Luyten was adopted here for two reasons: first, to preserve comparability with the error estimates published for the west Atlantic and second, because this method is likely to overestimate the standard error and thus provide a conservative estimate of significance. The reader is referred to FLIERL and MCWILLIAMS (1977) for a fuller discussion of the inadequacies and assumptions of error estimation via this technique.

The standard error estimates for mean u and v components are listed for the majority of records in Table 1. Figure 2 describes the amplitude of mean u and v estimates as a percentage of their standard errors in each 0.5 cm s^{-1} band of mean speed for 85 of these records. Only in the lowest mean speed category (0–0.5 cm s^{-1}) is the mean consistently lower than the standard error, though it should be remembered that some 38 to 40% of available records fall in this band. [Fig. 1].

3. GEOGRAPHICAL VARIATION OF DOMINANT TIME SCALE

The two general characteristics of eastern basin records thus far identified are that (a) deep mean flows are relatively weak (Fig. 1) and nowhere approach the highest mean speeds attained

TABLE 2. EDDY KINETIC ENERGIES K_i ($cm^2 s^{-2}$) IN FOUR RANGES OF PERIODS (COLUMNS 4 TO 7) FOR SELECTED SITES AND DEPTHS ON A NORTH–SOUTH SECTION [NEADS 6(3) TO 81–16] AND SOME POSITIONS EAST AND WEST OF THIS SECTION. DEPTH LEVELS 0, 1 AND 2 INDICATE HEIGHTS ABOVE BOTTOM ≥ 1,500 m, 0 (1,000 m) AND ≤ 5,000 m, RESPECTIVELY. COLUMN 8 GIVES $K_1/\Sigma K_i$ THE AMOUNT OF ENERGY CONTAINED IN THE LOW FREQUENCY RANGE COMPARED TO THE TOTAL ENERGY CONTENT IN ALL FOUR BANDS. R GIVES THE RATIO OF ENERGY CONTENT IN THE SUB-MESOSCALE BANDS 2 AND 3 TO THAT OF THE SAME BANDS AT THE LEVEL ABOVE. IN COLUMN 10, RECORD LENGTHS MARKED * WERE SUPPLEMENTED WITH ZEROES TO BRING THEM TO 256 DAY DURATION (SEE TABLE 1 FOR EXACT POSITIONS AND WATER DEPTHS)

Identifier	Level	Depth (m)	K_1 512–46.5 days	K_2 46.5–14.6 days	K_3 14.6–7.0 days	K_4 7.0–2.0 days	$K_1/\Sigma K_i$ %	R	Record length used (days)
NEADS 6(3)	1	3047	4.33	5.49	6.42	1.14	25		
	2	4074	4.35	7.54	9.97	1.83	18	1.5	256
N	1	3984	7.72	4.23	0.27	0.12	63		
	2	4704	7.22	4.19	0.37	0.25	60	1.0	256
O	1	3990	3.16	1.45	0.21	0.08	65		
	2	4770	2.80	1.51	0.34	0.17	58	1.1	256
NEADS 5	1	4050	0.37	0.27	0.05	0.03	51		
	2	4710	0.40	0.31	0.14	0.08	43	1.4	256
NEADS 2.5	1	4050	0.08	0.05	0.03	0.03	42		242*
NEADS 2	0	3168	0.48	0.10	0.05	0.05	71		512
	1	4181	0.59	0.13	0.07	0.08	68	1.3	256
	2	5079	-	0.21	0.11	0.06	-	1.5	128
NEADS 1	0	3050	2.19	0.27	0.04	0.04	86		256
	2	4780	-	0.52	0.31	0.19	-	2.7	320
81-16	0	3195	0.33	0.15	0.03	0.03	73		252*
	1	4246	1.58	0.33	0.03	0.03	80	2.0	252*
	2	5246	1.54	0.36	0.08	0.08	75	1.2	252*
NEADS 7	0	3000	0.78	0.24	0.03	0.13	66		256
	1	4000	0.95	0.62	0.09	0.08	55	2.6	640
81-03	2	3945	1.13	0.48	0.36	0.36	49		256
265	1	2520	2.25	0.61	0.27	0.26	66		640
NEADS 4	2	3500	1.23	0.13	0.05	0.06	70		640
NEADS 3	0	3000	4.02	0.27	0.05	0.02	85		256
81-18	1	3480	1.92	0.91	0.27	0.07	61		252*
	2	4461	3.92	4.77	1.06	0.41	39	4.9	252*
81-14	1	3935	-	0.38	0.41	0.11	-		128
	2	4862	1.88	0.57	0.21	0.10	68	1.0	256

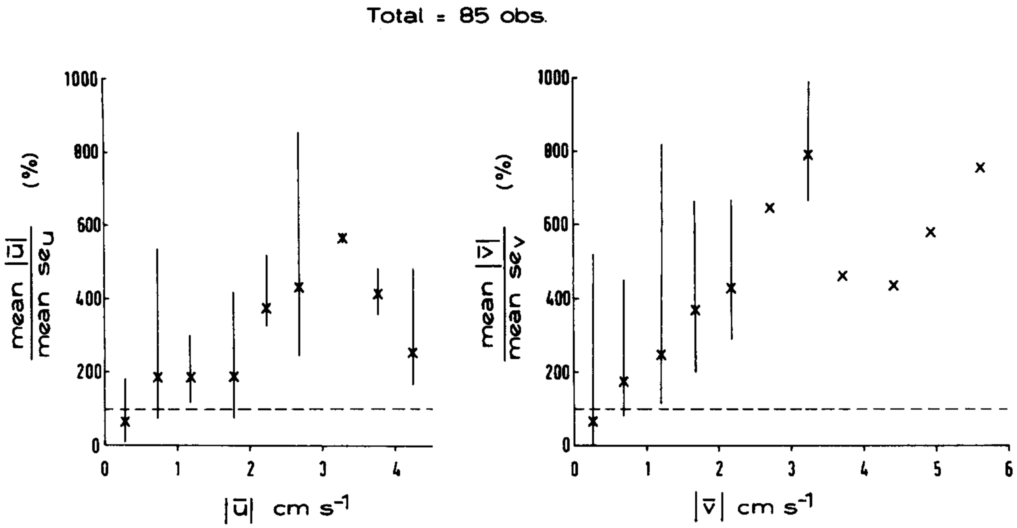

FIG. 2. Mean $|\bar{u}|$ and mean $|\bar{v}|$ expressed as percentage of their respective standard errors in each 0.5 cm s^{-1} band of mean speed. Bars indicate total range of values. Standard errors exceed the means for points below the dashed line.

in the western basin (DICKSON, 1983; HOGG, 1983), (b) the weakest category of these mean flows tend to be smaller than their standard error estimates (Fig. 2).

However, apart from these generalisations, reliable means can still be expected to occur in areas where mean flows are at their strongest and where records are dominated by high frequency motions rather than by long time-scales.

Figure 1 has provided information on the first of these characteristics in showing that mean speeds greater than 1 cm s^{-1} have been encountered predominantly north of 45°N (unshaded in Fig. 1).

The geographical distribution of dominant time scales shows a tendency for the longest time scales to prevail in the southern interior sites, and for them to become progressively shorter going northwards to the head of the Porcupine Abyssal Plain.

This point may be illustrated by spectra from mooring sites which cover the full breadth and latitudinal extent of the north-eastern basin. For 27 such records the fluctuation kinetic energy K_i was calculated for four period-ranges similar to those employed by SCHMITZ and HOGG (1978):

K_1 period range 512–46.5 days

K_2 period range 46.5–14.6 days

K_3 period range 14.6–7.0 days

K_4 period range 7.0–2.0 days.

The results are listed in Table 2, categorised (column 2) into 3 ranges of height above the bottom [$\geqslant$ 1,500 m, 0 (1,000 m) and $\leqslant$ 500 m]. As is the case for total eddy kinetic energy, K_E, (DICKSON, 1983) the energy content in individual frequency bands appears lower in the north-eastern Atlantic than in the north-western (cf. SCHMITZ, 1978, SCHMITZ and HOGG, 1978); [note that $K_E \neq \Sigma_{i=1}^{4} K_i$ since the latter is based on a restricted record length (Table 2, column 10) and a restricted band of frequencies.]

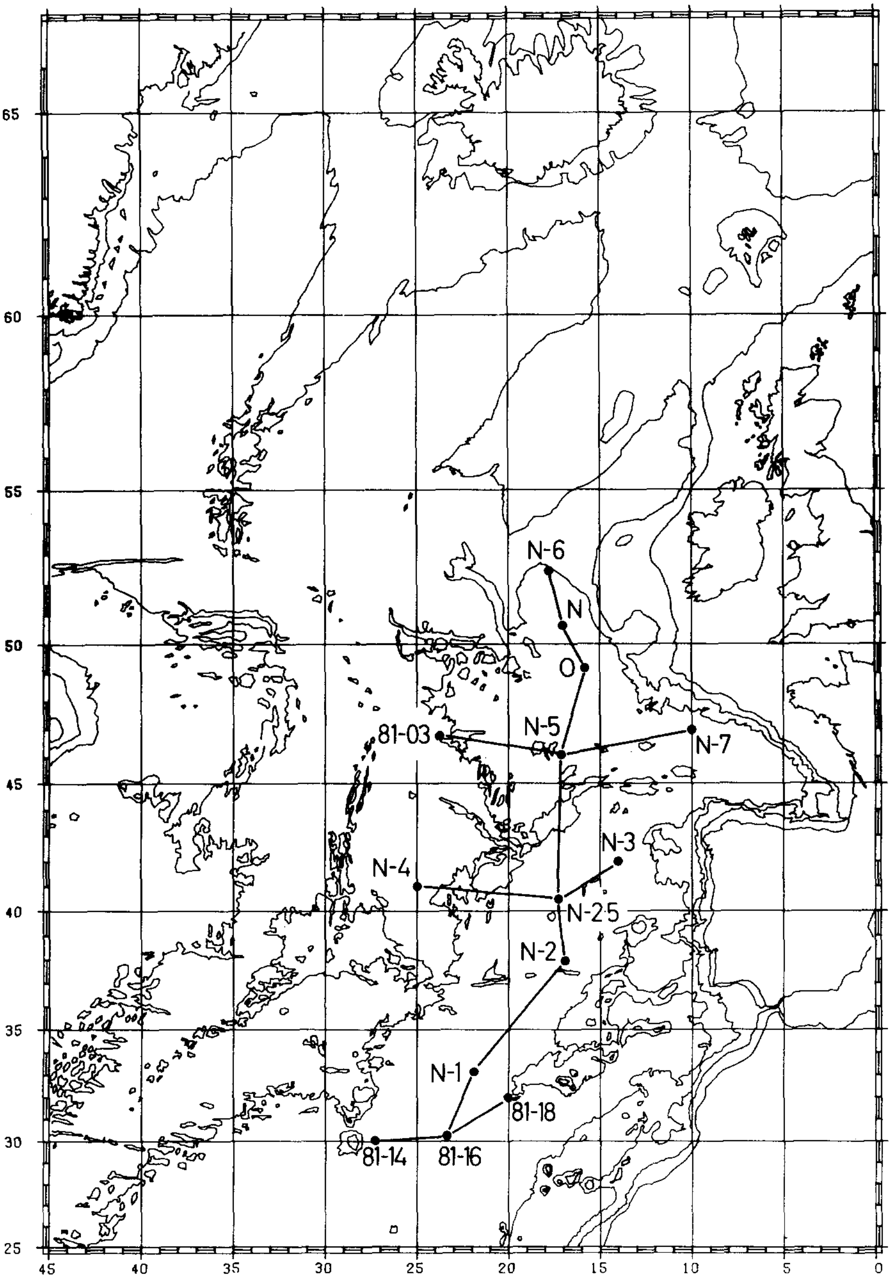

FIG. 3. Transects of moorings for which spectra are described in Fig. 4.

Even before these results are normalised for differences in band-width, some general trends in the regional- and depth-distribution of dominant time-scales are apparent in Table 2. K_4 is unimportant everywhere and over all depths considered; the energy content in sub-mesoscale bands $K_2 + K_3$ tends to increase with increasing depth (the values of R in Table 2, column 9 are of order 1 or larger); and the *relative* importance of K_1 to the total energy content in the

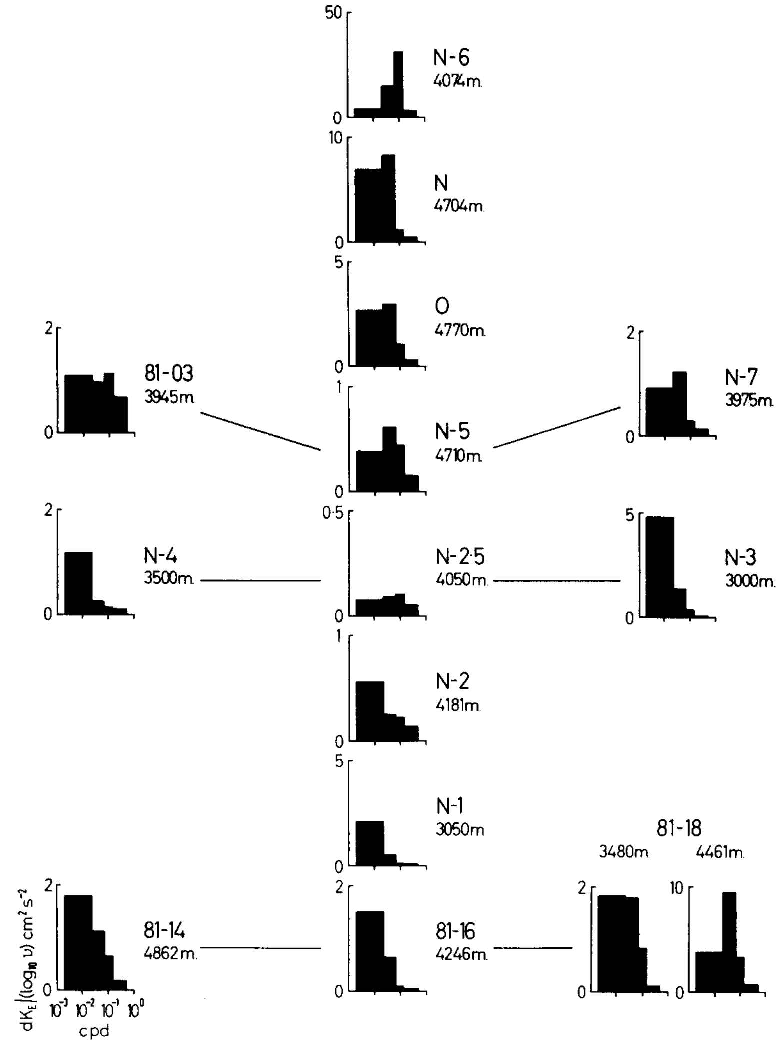

FIG. 4. Decadel kinetic energy frequency spectra, energy preserving by area, for 14 mooring sites in the deep eastern basin.

record $(\Sigma_{i=1}^{4} K_i)$ tends to increase southward and decrease marginally with depth. K_1 is of course the band which most severely influences uncertainties in the estimates of the means.

The important spatial changes in dominant time scale are more clearly seen however in Fig. 3 and 4 which display decadal kinetic energy frequency spectra, energy-preserving by area, (SCHMITZ and HOGG, 1978) for a representative subset of 15 of the 27 records listed in Table 2. As the location chart shows (Fig. 3), these records form a meridional transect along the deep axis of the basin from NEADS-6 in the north to mooring 81–16 in the Madeira Abyssal Plain, together with three shorter zonal sections running from the Mid-Atlantic Ridge towards the eastern margins of the basin at nominal latitudes of 46°, 41° and 30–32°N.

Here, no attempt is made to distinguish any detailed changes with depth or with distance from the seabed but simply to describe the first-order changes in spectral shape with latitude and longitude. For this purpose the spectra shown may be regarded as representative of any of

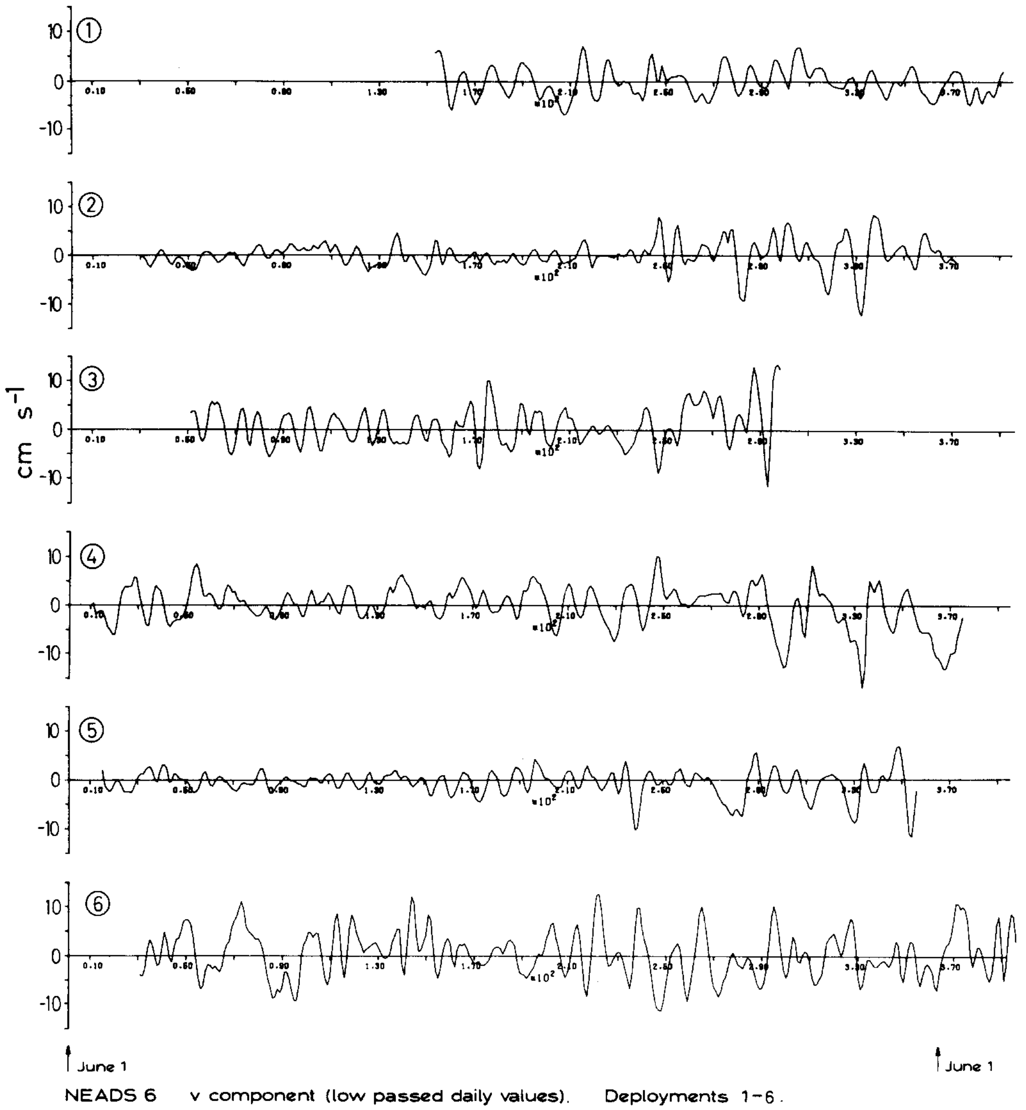

FIG. 5. Low-pass filtered time-series of daily mean north current component at ~ 3,050 m depth for 6 successive annual deployments of the NEADS-6 mooring (52°27′N 17°43′W). Elapsed days since June 1 each year are indicated.

the deep records from a given mooring with the exception of mooring 81-18 for which two spectra are illustrated.

In the north the NEADS-6 record from the Continental Rise at the mouth of the Rockall Trough is dominated by the shortest time scales, of ~ 10–15 day period. Their cause is attributed more to the characteristics of the site (bottom slope) than to its latitude, and the variations observed are thought analogous to those at site D where topographic Rossby waves are trapped to a similar bottom slope (THOMPSON, 1971, 1977). The spectrum from 4,074 m is nevertheless representative of a considerable depth layer in the lower water column. Figure 5 shows that a ~ 10 day periodicity has dominated the v component at ~ 3050 m over a record length approaching 6 yr.

Moving south, the spectra on the meridional transect to NEADS-5 and on the zonal transect at ~ 46°N show a lower-frequency dominance in bands 2 or 3, and this is again representative of records at least 1,000 m shallower than those shown. GOULD (1983) and DICKSON, GOULD, GURBUTT and KILLWORTH (1982) demonstrate that in the case of NEADS-5 the spectrum is made up of two seasonally-varying components – long period dominance in the summer and shorter period dominance due to atmospheric forcing during winter. Despite the good agreement in spectral shape in the examples and depth range shown, we can expect that this may not hold closer to the basin margins. Apart from topographic effects of the continental rise and slope already mentioned, both SCHMITZ and HOGG (1978) and DICKSON, GURBUTT and MEDLER (1980) describe markedly depth-dependent spectra (shifting to higher frequency dominance with increasing depth) in records from the northern and southern trenches of the Charlie Gibbs Fracture Zone of the Mid Atlantic Ridge, and Table 2 also includes one record from high on the flanks of the Ridge (mooring 265, 2,520 m) whose long-period dominance is inconsistent with the deeper records to its east.

Continuing south along the main meridional transect the NEADS-2.5 mooring in the Iberia Abyssal Plain – the least energetic deep site yet encountered in the eastern basin (DICKSON, 1983) – continues to show sub-mesoscale dominance at depth, but almost everywhere to the south of this site, and at the NEADS-3 and 4 moorings to its east and west, spectra become dominated by the longest accessible time scales; the few exceptions to this general rule are thought to be due to local topographic control, e.g. the near-bottom record at mooring 81-18 on the slopes of the Madeira Rise [Fig. 4].

Thus although the present data-coverage remains insufficient to distinguish fully or with any certainty between regional and local (e.g. topographic) effects on dominant time-scale, the available data set does at least suggest a consistent pattern of variation in the deepest layers of the northeastern basin. There, the tendency appears to be for time-scales to shorten with latitude from scales of hundreds of days in the south of the region to tens of days in the north.

4. CUMULATIVE AVERAGES OF u, v AND K_E

The preceding discussion has underlined two general (and at present poorly-based) tendencies in the available data; first, a progressive decrease in the dominant time-scale of variation northwards through the eastern basin from the ultra-long ("secular" in SCHMITZ, 1978) time-scales at the southern interior sites, to mesoscale or higher frequency dominance at the head of the Porcupine Abyssal Plain. Second, some tendency for the higher mean speeds to occur towards the north of the region.

If valid, these twin tendencies imply a more rapid establishment of statistically reliable means in the north than in the southern interior sites. To test the validity of this assumption, cumulative averages of u and v were calculated at 30 day increments for six of the longest deep records which cover the length and breadth of the eastern basin; NEADS-1 in the Madeira abyssal plain, NEADS-2 and 3 in the Iberia abyssal plain, NEADS-7 in the Biscay abyssal plain, mooring 265 of the Institut fur Meereskunde, University of Kiel (J MEINKE, *pers. comm.*) on the eastern flanks of the Mid Atlantic Ridge, and NEADS-6 from the continental rise at the southern entrance to the Rockall Trough (Fig. 6). These records, ranging in depth from 2,500 to 4,050 m, were selected for their exceptionally long duration. NEADS-6, is now in its 7th yr of deployment while two-year data sets are available from the remainder.

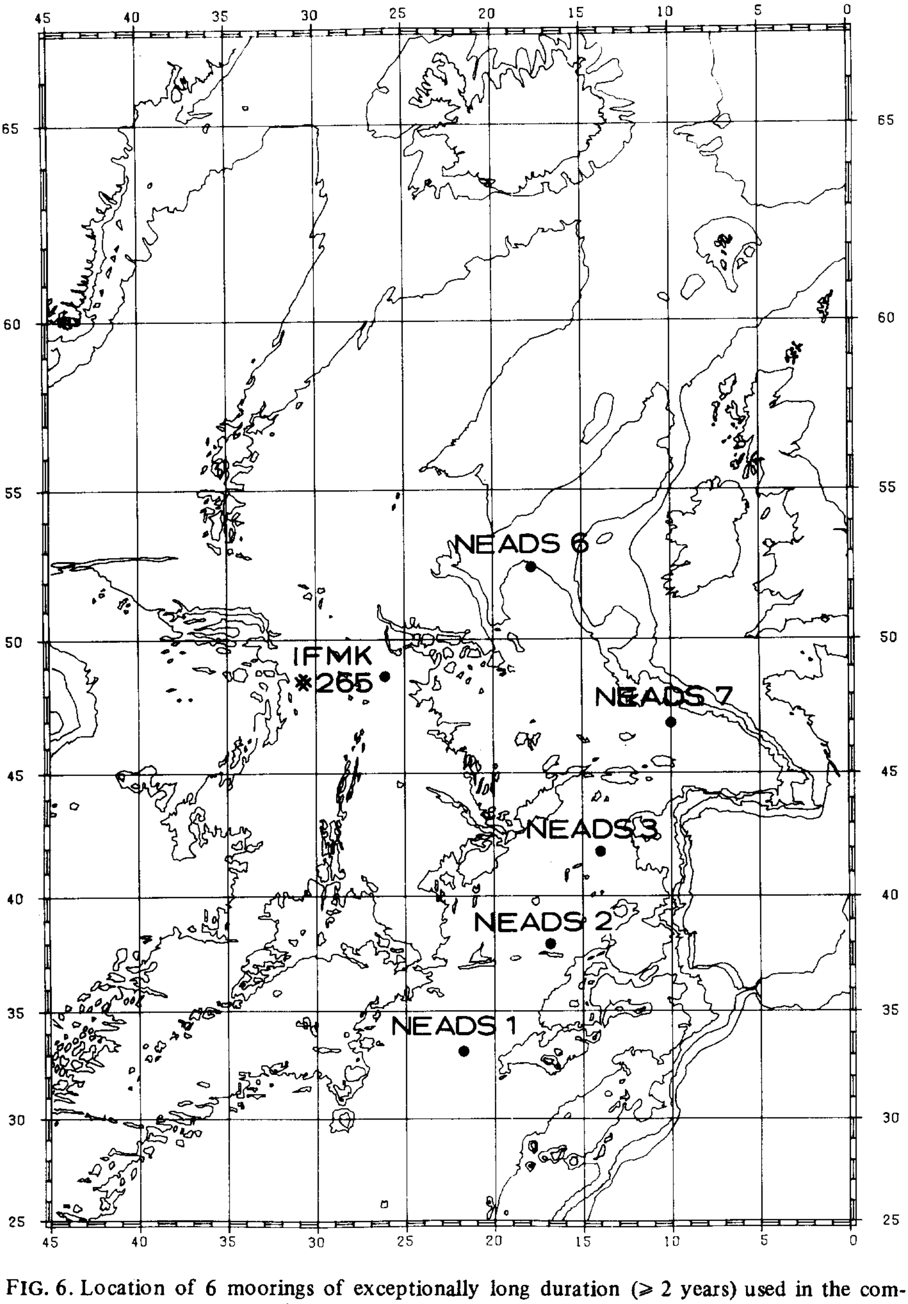

FIG. 6. Location of 6 moorings of exceptionally long duration (⩾ 2 years) used in the computation of cumulative-average flow statistics in Figs 7–9.

The cumulative averages of u and v, each stepping by 30 day increments of data are illustrated in Figs 7 and 8, and where major gaps in the time-series were encountered, these are indicated.

Though, arguably, the statistics seldom achieve true stationarity, the length of record required to achieve reasonably reliable statistics does appear to vary geographically in the expected

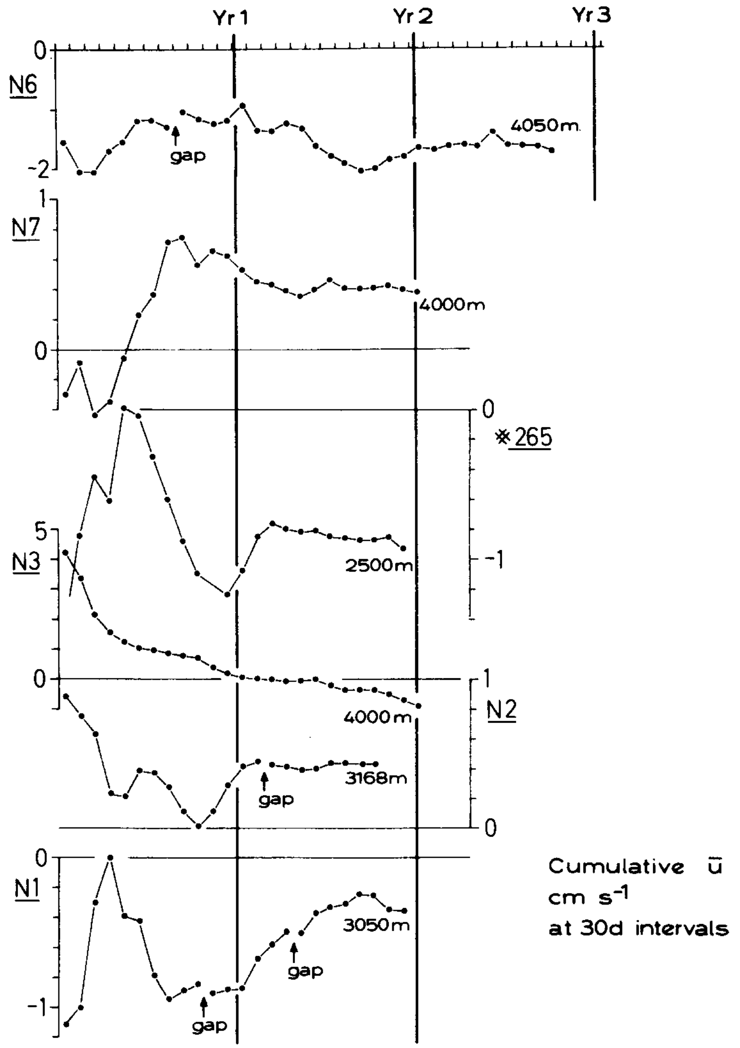

FIG. 7. Graphs of cumulative $\bar{u}$ (cm s^{-1}), each stepping by 30 day increments of data, for 6 long records from the deep eastern basin. Major gaps in the time-series are indicated.

sense. In the case of the northern NEADS-6 record which is characterised by the highest (10–15 days) dominant frequency of variation, a consistent estimate of the speed and direction of the mean flow is rather quickly achieved: the flow is westward throughout with a variable but minor north component of flow. At the other extreme the southern NEADS-1 record varies continuously in the amplitude of both the zonal and meridional components of flow, and it is unclear even at the full record length of 2 yr whether the "sense" of the mean circulation at this site has yet been adequately estimated. At intervening latitudes the indications are that reasonably reliable estimates of both the speed and direction of the mean flow require a minimum record length of some 9–14 months. [Mooring 265, with an anomalously long dominant time-scale for its latitude (Section 3), is the slowest of this intermediate group of records to reach a stable mean.]

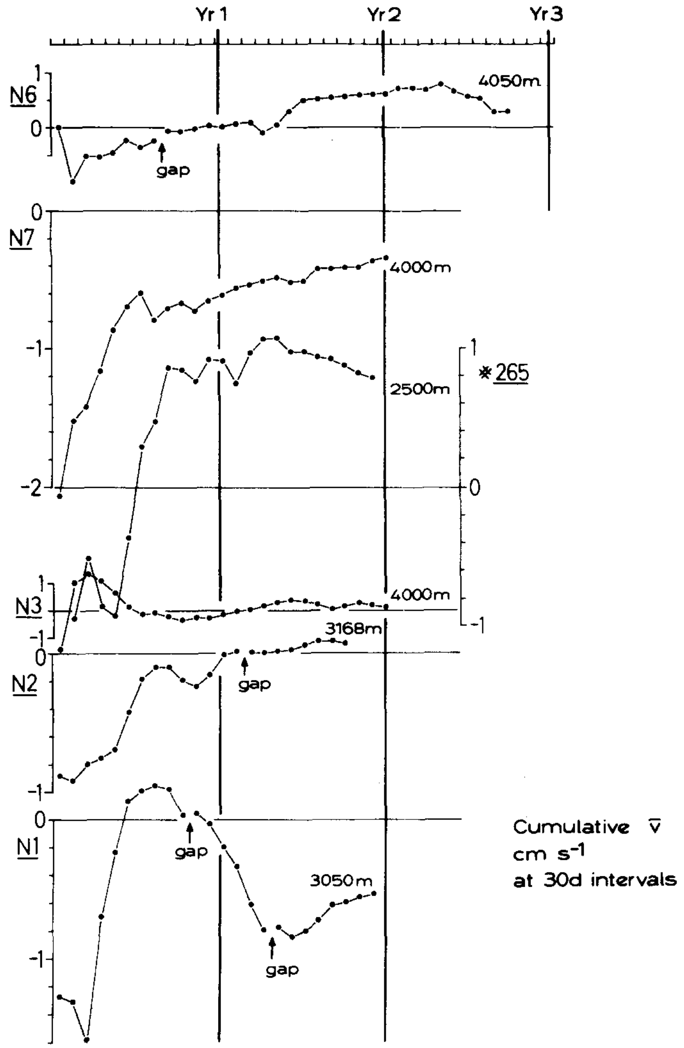

FIG. 8. Graphs of cumulative $\bar{v}$ (cm s^{-1}), each stepping by 30 day increments of data, for 6 long records from the deep eastern basin. Major gaps in the time-series are indicated.

These results are tempered, inevitably, by the small number of ultra-long records on which they are based, by their often "gappy" nature and by the fact that they include (and to a variable degree) the effects of local topographic constraints on the flow field, not merely the effects of basin-wide variations in dominant time-scale. They do however provide some reassurance that the search for reliable means from ~ 1 yr records is not a pointless exercise in the deep eastern basin, even though, quite commonly, these means may be of little better than marginal statistical reliability unless aided by relatively strong flows, short time-scales of variation and some degree of topographic constraint. Since the mooring-durations were primarily designed to comment on the variances rather than the means, this point is of some importance. [Figure 9 confirms that as theoretically expected, the variances converge much more rapidly than the means towards reasonably steady average values; even at NEADS-1, this occurs within 6–9 months.]

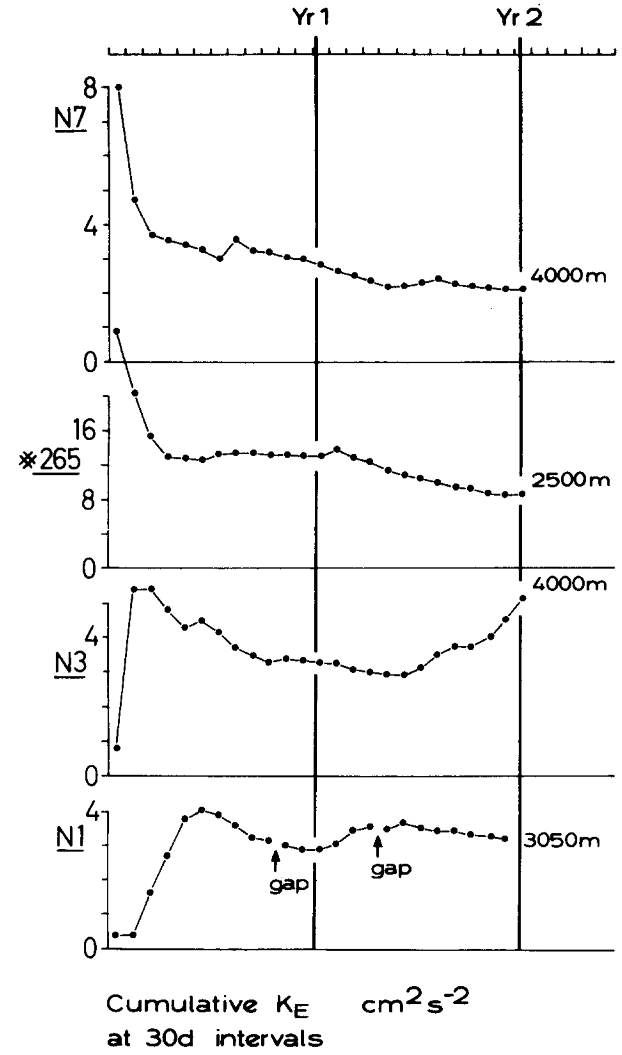

FIG. 9. Graphs of cumulative K_E ($cm^2 s^{-2}$), each stepping by 30 day increments of data, for 4 long records from the deep eastern basin. Major gaps in the time-series are indicated.

5. REGIONAL CIRCULATION PATTERNS

5.1. *The Porcupine Abyssal Plain*

Here, of the three regions to be considered, the mean flow vectors are the strongest, the data density is greatest, and the circulation pattern itself appears the most systematic (Fig. 10). We may even assume a degree of confidence in the reliability of certain elements of this pattern. For example, since its existence was first postulated (SWALLOW, GOULD and SAUNDERS, 1977; ELLETT, DOOLEY and HILL, 1979), the presence of a north-going residual slope current along the European continental margin has been confirmed wherever direct measurements have been made and at whatever depth on the slope; the very recent results of the U.K.

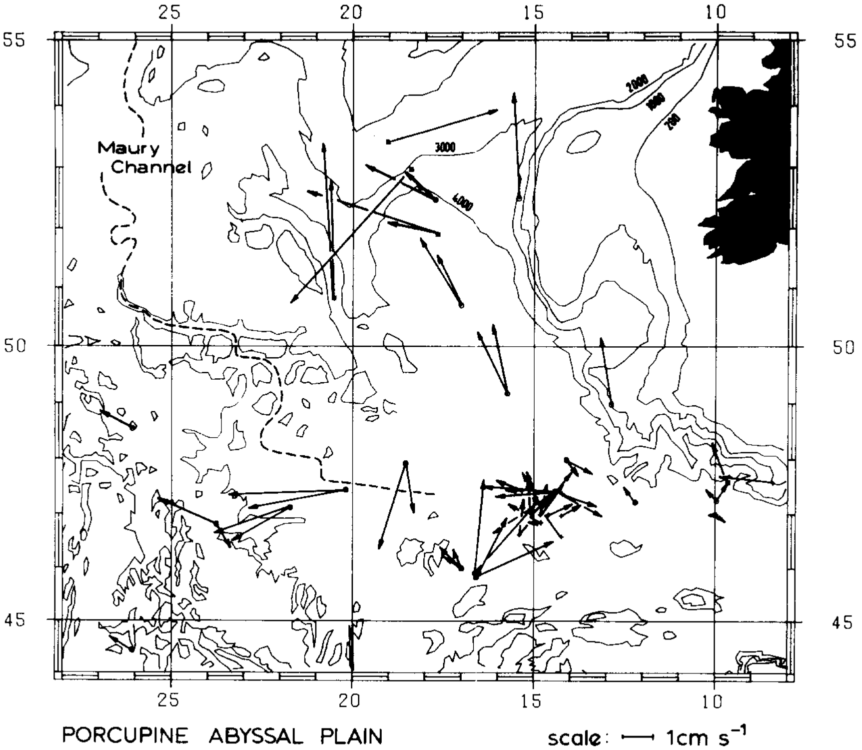

FIG. 10. Mean flow vectors for all available records > 2,000 m depth from the Porcupine Abyssal Plain and its surroundings.
[Note that Table 1 also lists 10 records from the Charlie–Gibbs Fracture Zone, to the west of this chart.]

Continental Slope Experiment (CONSLEX) have reinforced this conclusion. In the past, most records have been from the upper part of the slope, and are therefore not considered here, but the four vectors shown at depths of 2,000–2,500 m between the Celtic Sea slope and the slope west of Porcupine Bank are thought to provide a reliable indication that the northgoing flow blanketing the slope extends to these depths also.

In the deep water to the west of the slope, residual current vectors from a range of years suggest a fairly systematic circulation which flows in a cyclonic sense, northward at 1–2 cm s^{-1} up the central part of the abyssal plain, to turn westward and southwestward as the basin shoals in the north and thence southward or westward along the eastern flanks of the Mid Atlantic Ridge. A gap in coverage from 47°–50°N at ~ 20°W prevents us from establishing the continuity or otherwise of this apparently cyclonic basin circulation, but it appears likely that at least a part of the flow leaves the basin as an offshoot to the west or northwest to enter the South Icelandic Basin as a thin but steady and relatively strong near-bottom current. Mooring 82-11 at 50°50′N 20°31′W occupied the deepest part of the gap between the Mid Atlantic Ridge and the tail of Rockall Bank and showed a steady bottom-intensified flow of ~ 5 cm s^{-1} along the axis of the trench over a deployment of 1 yr duration. This mooring was laid in response to preliminary data from the 50°N TTO section which suggested that a near-bottom flow might occur persistently within the narrow Maury Channel leading WNW to the Icelandic Basin. (CLAES ROOTH, U. Miami, *pers. comm.*). The results of mooring 82-11 from the alternative deep channel close by to the north confirm Rooth's interpretation of the TTO data as evidence of a near-bottom flow through this gap from a source further east.

Needless to say there remain exceptions to the oversimplified picture of the circulation just described, though these are not necessarily unexpected. The apparently anomalous northeastward flow at 53°25'N 19°02'W on the south slope of Rockall Bank stems from a full-depth 6-mooring array across this slope. Records above ~ 2,000 m depth (not shown here) were directed northeastward into the Rockall Trough while those below 2,500 m showed west or southwest flows. The record in question, from 2,450 m depth, is evidently part of the former group.

5.2. *The Iberia Abyssal Plain*

The Porcupine Abyssal Plain is partially closed-off to the south by the topographic barrier of the Azores–Biscay Rise. South of this Rise and north of the zonal Azores–Portugal ridge (~ 37°N), the deep flows circulating around the Iberia Abyssal Plain and flanks of the Mid Atlantic Ridge to its west are, arguably, not without "system" (Fig. 11) though the sparseness of the present coverage and the general weakness of the residual flows would argue against describing this circulation as of anything other than marginal reliability.

The deepest inflow to the northeastern basin that has been identified to date takes place through the Discovery Gap of > 4700 m sill depth at 37°25'N 15°45'W in the Azores–Portugal ridge. Table 1 lists only one record from this gap (mooring 310) where a northeastward residual of 3.8 cm s^{-1} was observed close to the bottom over a record length of 340 days. Very recently a 6-mooring array has been recovered from the gap (P. M. Saunders, IOS Wormley, *pers. comm.*), which should provide an estimate of the transport of this important connecting flow between the basins.

No records are yet available from sites close to the Iberian Slope but further offshore, the NEADS 3 and 2.5 sites on the Iberia Abyssal Plain give some indication that the deep mean

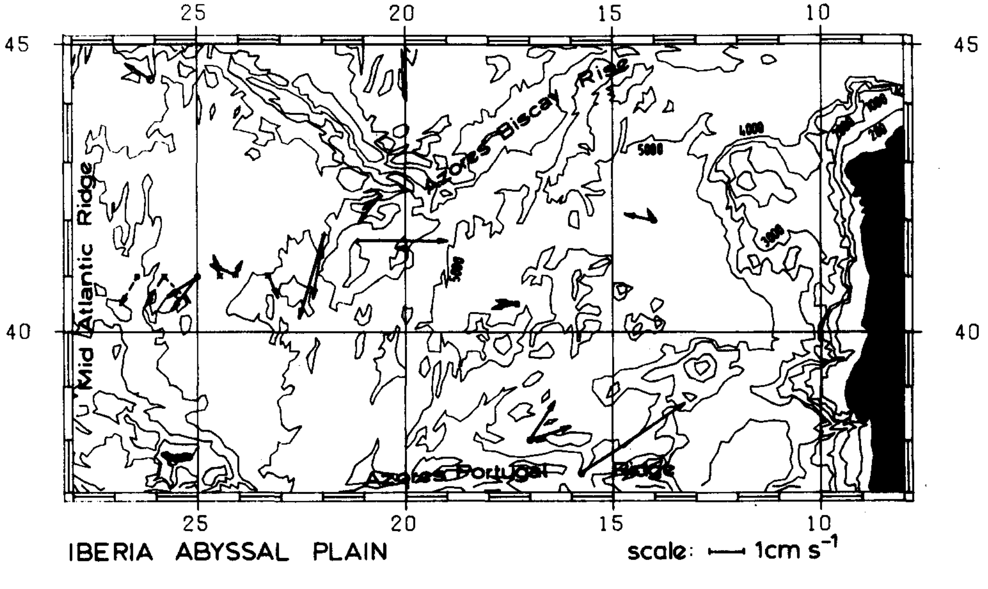

FIG. 11. Mean flow vectors for all available records > 2,000 m depth from the Iberia Abyssal Plain and its surroundings.

flow tends to run weakly westward with the basin topography towards the Mid Atlantic Ridge. There, the indications are of a predominantly southward flow along the flanks of the Ridge at depths ranging from 2,300–4,100 m, and at mean speeds of $\sim 0.5–2.5\ cm\ s^{-1}$. Of the exceptions shown, the anomalous eastward vector at mooring 80-16 (41°39'N 21°09'W) can be discounted; it lies on an east–west-trending slope at the northern margin of a seamount and thus could hardly contribute to the general southward pattern of flow in this area.

Finally along the northern slopes of the Azores–Portugal ridge, three records from the NEADS-2 mooring at 37°59'N 16°54'W provide at least some indication of an eastward or northeastward return flow along the southern margin of the Iberia plain. Mean speeds are $0.4–1.3\ cm\ s^{-1}$ intensifying towards the bottom over a depth range of 3,168–5,079 m (2382–471 m above the bed).

The apparent simplicity of this deep circulation pattern may of course be attributable to the sparseness of observations; nevertheless the deep cyclonic gyre indicated here is justified at present as being the simplest pattern which can be fitted to the existing data. One particular deficiency of the data set is the complete lack of information on connecting flows between the Iberia and Porcupine/Biscay Abyssal Plains; in July 1983 however eight moorings were laid by MAFF across the three deepest gaps in the northern Azores–Biscay Rise (including the Theta Gap) and their results are awaited with interest.

5.3. *The Madeira Abyssal Plain*

Figure 12 describes mean flow vectors for all records recovered to date from the latitude of the Great Meteor Seamount (G.M.S.) to that of the Azores–Portugal ridge. (Note that the Polymode IIIB results and those from the French CV1 and CV2 sites, far to the south and west are listed in Table 1, but are not included here).

The sparseness of results in a region of such complex topography rules out any meaningful discussion of a deep mean circulation pattern, and questions of the reliability or otherwise of these measurements must be restricted to individual records which are of long duration and indicate relatively stable flows. The "stability factor" statistics listed in Table 1 are the ratios of mean vector to mean scalar speeds in each record, expressed as a percentage, and provide this measure of directional stability.

Only three of the records from this region fall in this category, and both of the moorings involved suggest increasingly stable flow-directions towards the bottom.

At the NEADS-11 site at 34°50'N 23°00'W, stability factors increase from 56% at 3,030 m to 92% at 4,720 m (435 m above the bed) over a record-length of 214 days. At mooring 81-16 (30°20'N 23°22'W) in the Madeira Abyssal Plain the corresponding increase is from 57% at 3195 m to 73% at 4246 m and 75% at 5246 m (50 m above the bottom). These three directionally-stable records are also among the most vigorous encountered in this region of the eastern basin, ranging from a northeastward residual of $3.2\ cm\ s^{-1}$ in the deep NEADS-11 record, to values of 1.8 and $1.9\ cm\ s^{-1}$ (also north-eastward) in the deep records from 81-16. Both the speed of the mean flow and its increasing directional stability with depth suggest that these deep records owe their abnormal "realiability" (for this area) to some degree of local topographic constraint. Detailed bathymetric control is not yet available for the NEADS-11 site but precise bathymetric survey of the area immediately to the north of 81-16 (DUIN and KUIJPERS, 1983) indicates the presence of a scarp trending NNE from the position of the mooring.

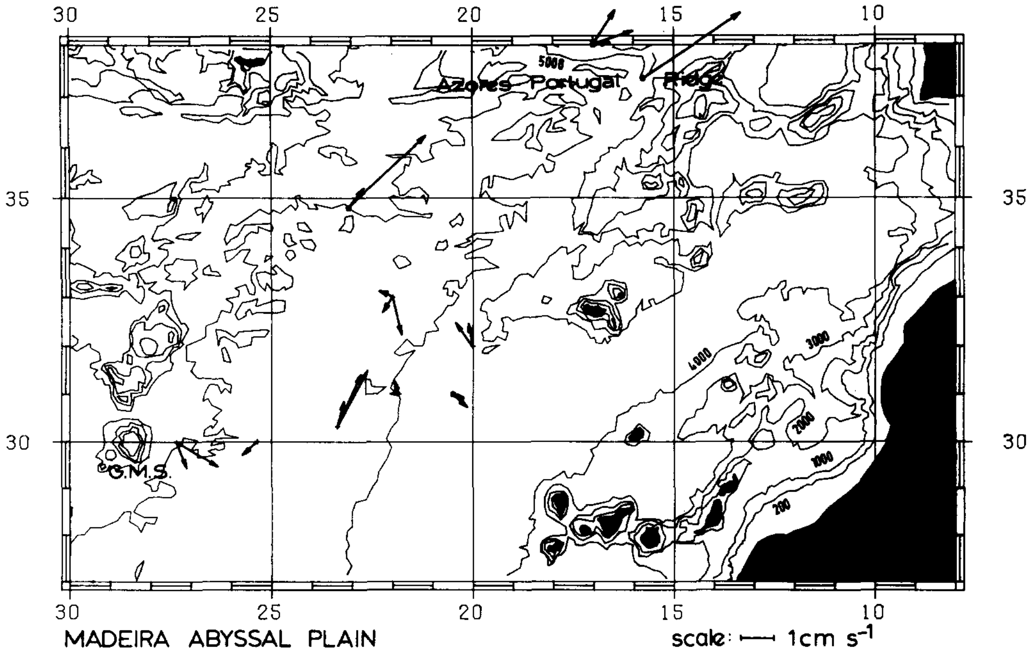

FIG. 12. Mean flow vectors for all available records > 2,000 m depth from the Madeira Abyssal Plain and its surroundings.
[Note that Table 1 lists a further 8 records from POLYMODE IIIB, CV1 and CV2 to the south and west of this chart.

6. COMPARISON WITH INDIRECT ESTIMATES OF THE FLOW FIELD

Of the numerous recent studies which have attempted to describe the deep circulation of the North Atlantic or its eastern basin from a variety of indirect evidence, some compare well with the results of deep current meter records. For example, both the deep southward western boundary current in the Atlantic and the broad interior poleward flows required by the thermohaline circulation schemes of STOMMEL (1958), STOMMEL and ARONS (1960 a, b) and VERONIS (1978) appear to be confirmed in recent direct measurements from the west Atlantic (e.g. JENKINS and RHINES, 1980; HOGG, 1983) and northeastern Pacific (WARREN and OWENS, this volume).

However, a range of other circulation schemes based on the dynamic method and its assumptions (e.g. IVERS, 1975; WUNSCH and GRANT, 1982; SAUNDERS, 1982) remain not only untested against direct observations, but are arguably untestable. To quote Wunsch and Grant (p1): "... neither these model circulations nor any other circulation pattern based upon the existing data can be regarded as actually representing the true time average ocean circulation because the data are aliased in time; the frequency/wavenumber spectrum of the ocean is inadequately known to determine the resulting errors" and later (pp. 55–56): "Our results share a major shortcoming with every one of the previous attempts at deducing the general circulation of the North Atlantic from the dynamic method. They are essentially untestable. Any detail of the circulation inferred from any given data set which differs from someone else's scheme may have represented properly the ocean at that time ... An attempt to "check" one of them by new direct observations is doomed to failure because there will be real observed differences and it will be impossible to tell whether either the new or old data sets represent a transient state or the very long-term average flow."

Whether due to deficiencies in either data set or to the effect of aliasing in time, the deep circulation scheme proposed by Wunsch and Grant for the deep eastern basin (e.g. their Fig. 16 a–c) appears to bear as little resemblance to the circulation which we describe as their western basin scheme bears to the direct measurements described by HOGG (1983). It is idle to speculate which version is "better"; current measurements of ~ 1 yr duration are not free from aliasing as this paper has been at some pains to show.

A more profitable question is whether the results of deep direct current measurements from the eastern basin can narrow-down the choice of assumptions involved in using the dynamic method in this region. One general characteristic of these records, which may be of value to the choice of a reference level, is the fact that residual currents show some tendency towards bottom intensification. Table 1 lists 43 moorings which have pairs of instruments in the deep layer and where the deeper instrument lies within a few hundred metres of the bottom [NEADS-2.5 and 3 are ignored]. The percentage change in mean residual current speed normalised per 1,000 m increase in depth for these records is shown as a histogram in Fig. 13. Thirty-four out of 43 of these record-pairs show an increase in current speed with depth, the mean change being + 67%.

The point here is not to suggest that bottom intensification is a reliable tendency in the present data set, but to suggest that it would be unwise to assume the reverse – that current speeds decrease towards a level of no motion in the near bottom layer.

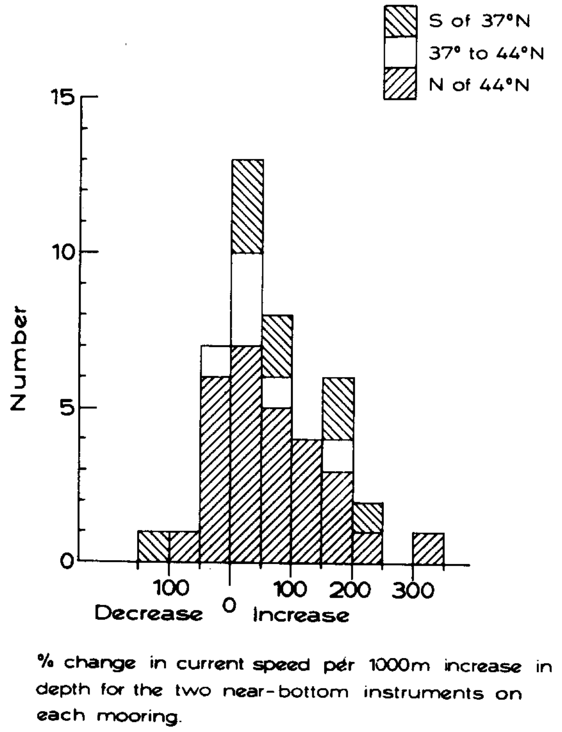

FIG. 13. Historgram of percentage change of mean current speed per 1,000 m increase in depth for near-bottom pairs of instruments.

SAUNDERS (1982) shows that the *section-average* vertical structure of relative geostrophic current velocity takes the form of "remarkably similar reverse-S shape profiles" on zonal sections of the eastern basin from 32° to 53°N. If so then clearly, as a basin-wide average, assumptions of a deep level of no net meridional motion can still be justified if we also assume a virtually closed circulation in the deep layer; but the growing conclusion that the deep eastern basin is ventilated from the south (e.g. BROEKER and PENG, 1982; MANTYLA and REID, 1983) leaves open the possibility that in the basin-wide average also there may be a net near-bottom intensification of flow and hence a net northward drift. The validiation of this point by means of direct measurements however must await a considerable future expansion of the present Eulerian data-set.

7. SUMMARY AND CONCLUSIONS

The accumulated data set of 131 long-term current meter records has been used to provide estimates of the mean circulation and their corresponding standard errors for the deep (> 2,000 m) layer of the eastern North Atlantic. The two questions to be addressed were first, whether a mean flow exists and second whether it can be reliably demonstrated in our relatively short records which were primarily designed to assess the variances rather than the means. This analysis suggests the following tentative conclusions regarding the flow field in this depth-layer of the eastern basin:

(a) Mean speeds are weak relative to the published results for the western basin. 45% of all record-mean vectors are weaker than 1 cm s^{-1}.

(b) At their weakest (< 0.5 cm s^{-1}) mean speeds tend to be smaller than their corresponding standard error estimates.

(c) Most mean speeds > 1 cm s^{-1} have been observed in the north of the basin, north of 45°N.

(d) There appears to be a progressive decrease in the dominant variability time scales northward through the deep eastern basin, from scales of hundreds of days at the southern interior sites to mesoscale or higher frequency (a few tens of days) dominance at the head of the Porcupine Abyssal Plain. This latitudinal pattern may be disrupted locally by topographic effects, especially at the basin margins.

(e) A majority of near-bottom records show some degree of bottom-intensification.

(f) Mean flow estimates are suggested to be most reliable in the north of the region where the strongest mean flows tend to coincide with the shortest time scales of variability.

(g) The most dependable element of the observed circulation is suggested to be the northward slope current along the continental margin of the Biscay and Porcupine Abyssal Plains. Steady northward mean flows of 1.4–3.4 cm s^{-1} are observed to at least 2500 m depth in this region (e.g. moorings 81-07, R, "Meriadzek Terr." and BIOGAS).

(h) Though major gaps in coverage remain, the deep circulation around the Porcupine Abyssal Plain appears to be both systematic and (relatively) vigorous. Flows are northwestward at 1–2 cm s^{-1} up the centre of the Plain but turn to the west and southwest as the basin shoals in the north to continue either southwards along the flanks of the Mid Atlantic Ridge or to pass westward as a near-bottom current towards the South Icelandic Basin. The latter flow was anticipated in interpretations of TTO section-data.

(i) A deep cyclonic gyre also appears to be the simplest flow pattern which fits the available data in that part of the basin between the Azores–Biscay Rise and the Azores–Portugal ridge, west of the Iberian Peninsula. The weak flows and sparse coverage however suggest that this cannot yet be described as a reliable result. More certain is the deep current which enters the Iberia Abyssal Plain from the south via the Discovery Gap, though the total transport through this gap has yet to be determined.

(j) South of the Azores–Portugal ridge observations are sparse and no systematic circulation is yet evident. The only "reliable" elements of the flow field in this region are the very few individual records where topographic constraints impose a degree of directional stability and perhaps also support some local intensification of the flow.

REFERENCES

ANON (1976) Report of SCOR Working Group 34. Meeting of the North East Atlantic Subgroup. pp. 28–30 [Annex III] In: *SCOR proceedings,* Volume 12, London, 63 pp.

BROEKER, W. S. and T.-H. PENG (1982) *Tracers in the sea,* Eldigio Press, Columbia Univ., Palisades New York, 690 pp.

DAVIS, R. E. (1976) Predictability of sea surface temperature and sea level pressure anomalies over the North Pacific Ocean. *Journal of Physical Oceanography,* 6 (3), 249–266.

DICKSON, R. R. (1983) Global summaries and intercomparisons: flow statistics from long-term current meter moorings. Chap. 15, pp. 278–353 In: *Eddies in marine science,* A. R. Robinson, editor, Springer-Verlag, Berlin Heidelberg, 609 pp.

DICKSON, R. R., P. A. GURBUTT and K. J. MEDLER (1980) Long-term water movements in the southern trough of the Charlie–Gibbs Fracture Zone. *Journal of Marine Research,* 38 (3), 571–583.

DICKSON, R. R., W. J. GOULD, P. A. GURBUTT and P. D. KILLWORTH (1982) A seasonal signal in ocean currents to abyssal depths. *Nature,* 295 (5846), 193–198.

DUIN, E. J. T. and A. KUIJPERS (1983) Geological Studies on Abyssal Plains in the North Atlantic. Rijks Geologische Dienst. Seabed Working Group Programmes, Progress Report 1982, 107 pp (Internal report, unpublished).

ELLETT, D. J., H. D. DOOLEY and H. W. HILL (1979) Is there a north-east Atlantic Slope Current? ICES CM 1979/C:35, 5 pp. (mimeo; unpublished ms).

FLIERL, G. R. and J. C. MCWILLIAMS (1977) On the sampling requirement for measuring moments of eddy variability. *Journal of Marine Research,* 35 (4), 797–820.

GOULD, W. J. (1983) Eastern North Atlantic. Ch. 7, pp. 145–157. In: *Eddies in marine science,* A. R. Robinson, editor, Springer-Verlag, Berlin Heidelberg, 609 pp.

HENDRY, R. M. (1982) On the structure of the Gulf Stream. *Journal of Marine Research,* 40(1), 119–142.

HOGG, N. G. (1983) A note on the deep circulation of the western North Atlantic: its nature and causes. *Deep-Sea Research,* 30(9A), 945–961.

IVERS, W. D. (1975) The deep circulation in the northern North Atlantic, with special reference to the Labrador Sea. Ph.D. Thesis U. Calif. San Diego 179 pp.

JENKINS, W. J. and P. B. RHINES (1980) Tritium in the deep North Atlantic Ocean. *Nature,* 286, 877–880.

LUYTEN, J. R. (1982) Equatorial current measurements. I. Moored observations. *Journal of Marine Research,* 40 (1), 19–41.

MANTYLA, A. W. and J. L. REID (1983) Abyssal characteristics of the World Ocean waters. *Deep-Sea Research,* 30(8A), 805–833.

SAUNDERS, P. M. (1982) Circulation in the eastern North Atlantic. *Journal of Marine Research,* 40 (Suppl), 641–657.

SCHMITZ, W. J. JR. (1978) Observations of the vertical distribution of low frequency kinetic energy in the western North Atlantic. *Journal of Marine Research,* 36(2), 295–310.

SCHMITZ, W. J. JR. and N. G. HOGG (1978) Observations of energetic low-frequency current fluctuations in the Charlie-Gibbs Fracture Zone. *Journal of Marine Research,* 36(4), 725–734.

STOMMEL, H. (1958) The circulation of the abyss. *Scientific American,* 199, 85–90.

STOMMEL, H. and A. B. ARONS (1960a) On the abyssal circulation of the world ocean. I. Stationary flow pattern on a sphere. *Deep-Sea Research,* 6, 140–154.

STOMMEL, H. and A. B. ARONS (1960b) On the abyssal circulation of the world ocean II. An idealised model of the circulation pattern and amplitude in oceanic basins. *Deep-Sea Research,* 6, 217–233.

SWALLOW, J. C. (1975) Status of the problem of intercomparison of current meters. (Annex V) In: SCOR Proceedings, 12(2), 114–115.

SWALLOW, J. C., W. J. GOULD and P. M. SAUNDERS (1977) Evidence for a poleward eastern boundary current in the North Atlantic Ocean. ICES CM 1977/C:32 16 pp (mimeo; unpublished ms).

THOMPSON, R. O. R. Y. (1971) Topographic Rossby waves at a site north of the Gulf Stream. *Deep-Sea Research,* 18, 1–19.

THOMPSON, R. O. R. Y. (1977) observations of Rossby waves near site D. *Progress in Oceanography*, 7(4), 135–162.

VERONIS, G. (1978) Model of world ocean circulation. III. Thermally and wind driven. *Journal of Marine Research*, **36** (1), 1–44.

WARREN, B. A. and W. B. OWENS (1985) Some preliminary results concerning deep northern boundary currents in the North Pacific. *Progress in Oceanography*, **14**, 537–551.

WUNSCH, C. and B. GRANT (1982) Towards the general circulation of the North Atlantic Ocean. *Progress in Oceanography*, **11**, 1–59.